Pergamon

Int. J. Heat Mass Transfer. Vol. 39, No. 16, pp. 3519–3529, 1996

0017–9310/96 $15.00+0.00

PII: S0017-9310(96)00014-2

Convective heat transfer and pressure drop characteristics of various array configurations to simulate the cooling of electronic modules

B. A. JUBRAN, S. A. SWIETY and M. A. HAMDAN

Department of Mechanical Engineering, University of Jordan, Amman, Jordan

(*Received* 19 *April* 1994 *and in final form* 21 *April* 1995)

Abstract—This paper reports an experimental investigation to explore the effects of the size of modules, the presence of a cylindrical module and the missing module on the heat transfer coefficient and pressure drop characteristics of array configurations composed of individual rectangular modules for three different Reynolds numbers namely; 1690, 2250 and 2625. Generally, it was found that using different sizes or shapes of modules in an array configuration tends to increase the Nusselt number by as much as 40% for the rectangular module and 28% for the cylindrical module. The presence of a missing module in the array resulted in a 37% enhancement in the Nusselt number downstream the missing module. Pressure drop results indicate that large size modules tend to enhance the pressure drop at their row locations by as much as 15%, while the cylindrical module tends to attenuate the pressure drop especially at low Reynolds number. Copyright © 1996 Elsevier Science Ltd.

1. INTRODUCTION

Microminiaturization of electronic components for digital computers and the instrumentation of modern aircraft has resulted in complex circuits and highly dense electronic boards, characterized by a high rate of heat dissipation per unit of component area. The geometrical characteristics of electronic modules, as well as the way they are implanted on the board, play a significant role on the heat transfer rate and pressure drop from these modules.

Buller & Kilburn [1] investigated the convective heat transfer from single-rectangular modules. Five specimens were tested; three plain square modules and two square modules with finned heat sinks attached. A single correlation based on the Reynolds number and Nusselt number was obtained and found to fit the results within 15% for all five modules.

Sparrow *et al.* [2, 3] reported data for heat transfer and pressure drop for air flows in arrays of heat generating square modules located along one wall of a flat rectangular duct. The effect of missing modules, as well as the implantation of barriers at various locations, were investigated. It was found that an increase in heat transfer coefficient by as much as 40% is obtained when the missing module is located upstream of the module of interest. The use of barriers in the array was found to be effective in enhancing the heat transfer coefficient by a maximum factor of 2.

Sparrow *et al.* [4] investigated the per-module heat transfer coefficient for a uniform array of square modules with the presence of different height modules or missing modules. It was concluded that the variations in the heights of modules tend to enhance the heat transfer coefficient. Wirtz and Dykshoorn [5] investigated the heat transfer coefficient from modules similar to those used by Sparrow *et al.* [4]. The module is a square one of 2.54×2.54 cm^2 and 0.635 cm in height. The elements were implanted in a sparse array with gaps of 2.54 cm between the adjacent elements, in both streamwise and spanwise directions. Lehmann and Wirtz [6] reported a study on the effect of variations in the streamwise spacing and the component length on the convective heat transfer and the level of turbulence from rectangular mounted components in a channel flow.

Moffat *et al.* [7] described the experimental study of forced convection related to the thermal protection of individual elements in an air cooled array of electronic components. Heat transfer coefficient results and thermal wake function were presented for in-line arrays of cubical elements. Ratts *et al.* [8] presented an experimental study of internal flow modulation induced by vortex shedding from cylinder in cross-flow and its effect on cooling an array of chips. They concluded that the heat transfer coefficient increase of up to 82% can be obtained when cylinders are placed periodically above the back edge of each row of chips.

Hollworth and Fuller [9] measured experimentally the heat transfer coefficient, pressure drop characteristics and thermal wakes for a staggered array of air-cooled rectangular elements. Torikoshi *et al.* [10] investigated the heat transfer characteristics and air flow pattern of block type elements in arrays with

NOMENCLATURE

A_c	flow cross-section associated with the gap height S [m^2]
A_{surf}	modules exposed area [m^2]
B	element side length [m]
c_p	specific heat of air [kJ kg$^{-1}\cdot$K^{-1}]
C_p	the per-row pressure coefficient for nonuniform array configurations
C_{po}	the per-row pressure coefficient for uniform array configuration
E	input voltage to the elements heater [Volts]
H	elements height [m]
H_1	element height in the fourth and fifth rows in the array [m]
H_2	element height in the basic array configuration [m]
h	heat transfer coefficient [W m$^{-2}\cdot$K^{-1}]
I	input current of the elements heater [Amperes]
k_{air}	thermal conductivity of air [W]
L	module side length [m]
L_1	side length of the odd modules [m]
L_2	side length of the basic array configuration modules [m]
N	denotes downstream row number, or the total number of modules downstream of the module of interest
Nu	Nusselt number for non-uniform array configurations (hL/k_{air})
Nu_0	Nusselt number for uniform array configurations (hL/k_{air})
q	heat flux rate [W]
Re	Reynolds Number ($\dot{w}l/A_c v$)
S	test section channel height [m]
T_1	temperature of the first module just downstream of the active module [K]
T_{act}	surface temperature of the active module [K]
T_N	temperature of the module at the Nth row downstream the active module [K]
T_{ref}	reference temperature of the fluid [K]
V	mean velocity in the empty channel [m s^{-1}]
W_1	width of modules at the fourth and fifth rows [m]
W_2	width of modules of the basic array configuration [m]
$\dot{w}$	air flow rate through the channel, [m^3 s^{-1}].

Greek symbols

ν	kinematic viscosity for air [m^2 s^{-1}]
ρ	air density [kg m^{-3}]
θ	thermal wake function
θ_1	thermal wake function of the first module next to the active module
θ_N	thermal wake function at the module N along the channel in the same column as the active module.

Subscripts

a	air
act	active
conv	convection
ref	reference
S	based on the channel height.

uniform height and arrays in which there is an abrupt change in the module height. It was found that the per block Nusselt number decreased monotonically with increasing downstream distance. The abrupt changes in height tend to enhance the per block Nusselt number in the streamwise direction.

To the best of the authors' knowledge, it appears that most attention has been paid to the heat transfer and pressure drop characteristics related to array configurations based on square or cubical modules. The aim of the present work is to investigate the heat transfer and the pressure drop characteristics for array configurations based on rectangular or noncubical modules of various length, width and height dimensions. The effects of a missing module, as well as cylindrical shape module, on heat transfer enhancement and pressure drop have also been investigated.

2. EXPERIMENTAL RIG AND EXPERIMENTATION

The experimental set up in this investigation is basically a modified version of that used by Hollworth and Durbin [11]. The setup consists mainly of a suction type wind tunnel with maximum flow rate of 0.24 m^3 s^{-1}. The main body of the test section is a channel like box 2 m in length, 0.33 m in width and 0.04 m in height. The test section and the wind tunnel have been constructed from 3 mm sheet metal. The front side wall of the test section accommodates at its middle section a double glazing window to ease observation of the configurations during the tests. At the air intake side of the wind tunnel a bellmouth is attached, and a flow straightener is placed at the front as well as at the trailing edge of the wind tunnel test section with a gradual contraction, which is connected to a circular cross-section pipe of the fan, Fig. 1.

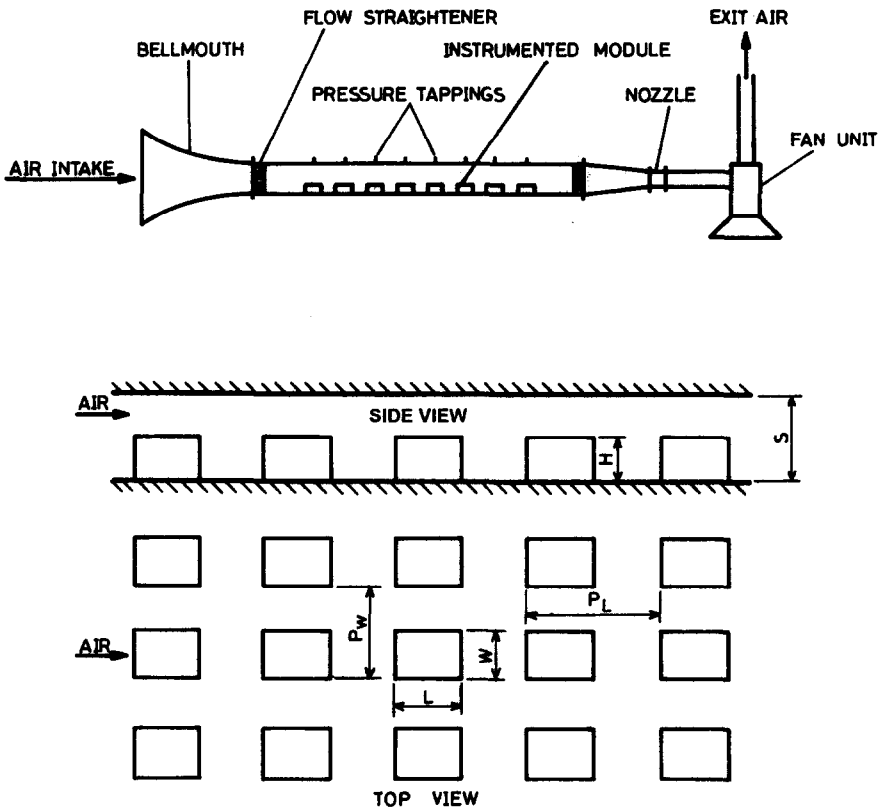

Fig. 1. Schematic diagram of the test rig.

The module array consists of individual rectangular elements of various dimensions manufactured from light metal aluminium alloy Duralumin. The modules in the array are arranged in eight rows each containing five elements. These modules are basically of three different heights; 5, 10 and 15 mm. For the purpose of this investigation, six basic dimensions of length and width were used. It should be pointed out that the long side of the module is always parallel to the airflow. For the 5 mm height module the dimensions are 15×10 mm. For the 10 mm height module, four different dimensions of 25×15 mm, 25×10 mm, 15×10 mm and 30×30 mm were used. For the 15 mm height module, two dimensions were obtained 25×15 mm, and 20×15 mm. Finally a cylindrical shape module 20 mm in diameter is implanted in one of the configurations. Figure 2(a) shows a typical basic array configuration in the test section. The parameters of the array configuration are; the height H, the length L and the width W of the modules with the subscript 1 denoting the dimensions for the modules in the fourth and fifth rows, while subscript 2 denotes the dimensions for the modules in any other row of the array. The uniform basic array configuration consists of modules each having 20 mm length, parallel to the direction of the flow, 15 mm width and 10 mm height. The spacing between the modules are 20 mm and 15 mm, in the streamwise and spanwise directions, respectively.

Each of the active modules is hollowed to the same size of the heater so as to accommodate a 22 Ω resistance heater, each rated at 2 Watts. The leads of the heaters are insulated, and are connected to a variable d.c. power supply. The module's power is held constant during the experiment, so that the per module heat flux is kept constant. The modules on the array test surface are fixed to a 3 mm balsa-wood which is fixed to a 12 mm wood sheet, Fig. 2(b). Each module in the array is threaded to accommodate a 3 mm screw, so that the modules are well attached to the base sheet. The position of the modules in the array can be varied in accordance with the desired configuration. Hence, it is possible to vary the modules spacing in the streamwise direction, as well as in the spanwise direction, and the tip to shroud clearance.

The steady-state temperature of the rectangular modules was obtained by embedding two copper–constantan thermocouples to the surface of each module of interest. All thermocouples were connected via the 3530 Orion-A data logger. The pressure drop across the array of the modules was determined by a total of 24 static pressure tappings mounted on the roof of the test section just over the module's array, and these were connected to an inclined manometer sensitive to the measurements of small deflections, as low as 0.05 mm of ethanol. This arrangement of pressure tapping enables the pressure drop to be obtained along the module's array, as well as at

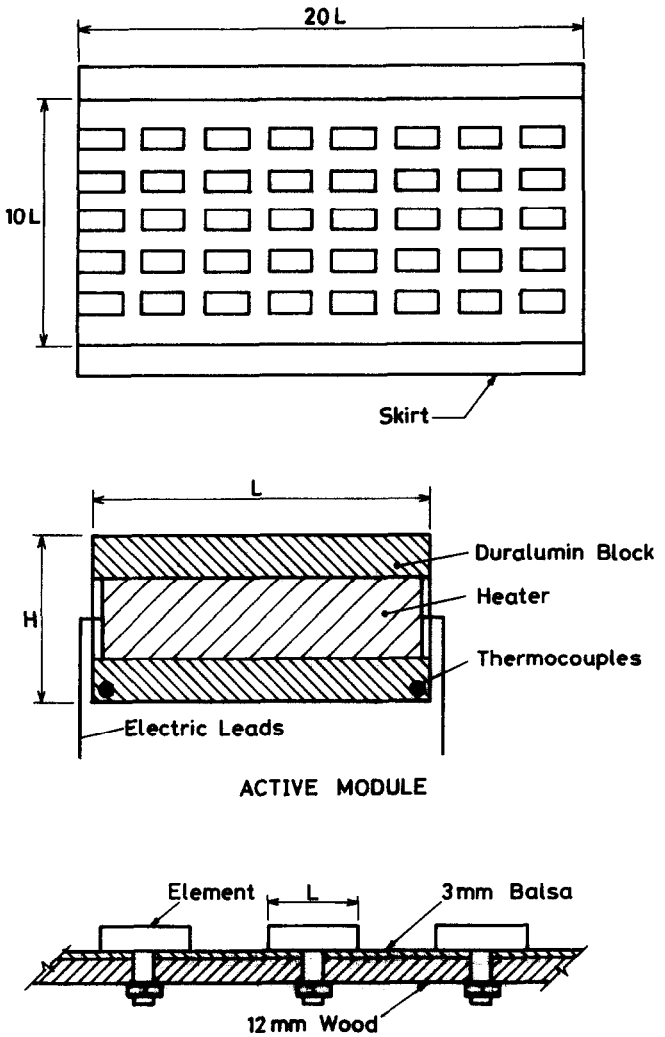

Fig. 2. Description of the general layout of the array.

locations before and after the array. At each row there exist three tappings and the average of these was taken as the static pressure at that location. The air flow rate was determined using a standard nozzle of 7.02 cm in diameter with a coefficient of discharge of 0.96 installed at the inlet section of the fan. Various flow rates were obtained by varying the speed of the fan.

Once the desired array configuration was installed in the test section, the fan was switched on with the right amount of air flow. The heaters were also switched on and the experimental setup was allowed to reach steady state, which was obtained after about 1 h. At this instant of time, the readings of temperature, input power, pressure drop and inlet temperature were recorded. The same procedure was repeated for different array configurations and flow rates.

3. DATA REDUCTION

The rate of convective heat transfer rate q was determined from the electrical power input to the module using

$$q = EI - \Delta q \tag{1}$$

where the term Δq is a small correction for conduction and radiation heat losses from the module. In order to minimize the radiation losses, the modules have been polished. The conduction heat losses have been minimized by fixing the modules to the balsa-wood plate. Hollworth and Durbin [11] reported that the conduction losses through such a surface never exceeds 4% of the heat input to the module. Furthermore, the same test surface was used by Wirtz and Dykshoorn [5] and it was shown, by thermal images technique, that very little spreading of heat was conducted into the balsa-wood surface adjacent to the heat dissipating modules. Assuming an emissivity of 0.12 for the module's surface, the correction factor combining both of these losses should not exceed 10% of the electrical power input.

The heat transfer coefficient was calculated from

$$h = \frac{q}{A_{\text{surf}}(T_{\text{act}} - T_{\text{ref}})} \tag{2}$$

where q is the heat input to the active module, A_{surf} is the five surface areas of the active module exposed to the air flow, T_{act} is the active module surface temperature, and T_{ref} is the steady-state of the passive modules at the first row of the array.

Thermal wake generation is experienced when an element in the array is heated. This thermal wake affects the modules downstream. The thermal wake function θ_N is defined as

$$\theta_N = \frac{T_N - T_{ref}}{T_{act} - T_{ref}} \tag{3}$$

where T_N is the temperature of the module of interest in the Nth row downstream of the active module, assuming that both of these modules are in the same column and within the column of modules of the array configuration, in the streamwise direction of the flow containing the heated element.

The temperature rise of the downstream passive module depends on the downstream distance from the active module. Taking the active module to be at $N = 0$, the dimensionless temperature rise of the first passive module downstream is expressed as

$$\theta_1 = \frac{T_1 - T_{ref}}{T_{act} - T_{ref}}. \tag{4}$$

The Reynolds number (Re) and Nusselt number (Nu) are calculated from

$$Re = \frac{\dot{w}L}{A_c v} \tag{5}$$

$$Nu = \frac{hL}{k_{air}} \tag{6}$$

where w, L, A_c, v and k_{air} are the air flow rate, the module side length that is parallel to the direction of the airflow, the cross-sectional area of the empty space over the modules, the kinematic viscosity of air, and the thermal conductivity of the air, respectively.

The presentations of the pressure drop results were classified into two groups. The first group is that for a basic uniform module array configuration, where a fully developed regime is established. In this region, the per-row pressure drop, Δp_{rpw}, is expressed in terms of the per-row pressure coefficient as

$$C_{po} = \frac{\Delta p_{row}}{1/2\rho V^2}, \tag{7}$$

where V is calculated as w/A_c and ρ is the air density. The second group of the pressure drop is that of the module array configurations of different lengths, heights and widths, where a substantial increase in pressure drop occurs and this is expressed in dimensionless form as C_p/C_{po}, where C_p represents the per-row pressure drop coefficient for the nonbasic array configuration having several rows, some of which may have cylinders, different size modules or empty spaces.

4. RESULTS AND DISCUSSIONS

Throughout the measurements made to establish the data presented in this paper, care was taken to note possible sources of error, and an error analysis based on the method of Kline and McClintock [12] was carried out. The error analysis indicated a $\pm 3\%$ uncertainty in the heat transfer coefficient and $\pm 2\%$ in the velocity. Tests were repeated a few times to ensure the repeatability of the results.

4.1. *Heat transfer results and discussion*

The row-by-row distribution of the per block *Nusselt* number for the basic uniform module array configuration is shown in Fig. 3, for three different values of Reynolds numbers; $Re = 1690$, 2250 and 2625. These results show that for all Re values, the maximum Nu is attained at the first row of modules, and decreases afterwards at the second row after which a 'hill-like' trend is observed at the third row, especially at the highest value of Re. This may be attributed to the separation of the impinging air flow at the first row of the modules of the array and the reattachment at the third row. Downstream of the third row of the modules, the Nu distribution seems to be almost independent of the row location. These rows are consequently considered as the fully developed region in the array. These results for the basic uniform module array configuration, together with those of Sparrow *et al.* [2], Wirtz and Dykshoorn [5], Torikoshi *et al.* [10] and Arvizu and Moffat [13], Fig. 4, were correlated using the following form:

$$Nu_0 = aRe^b \tag{8}$$

where Nu is the average value of Nusselt number in the fully developed region of the array. It is interesting to note that the value exponent b for all investigations that are shown in Fig. 4 is more or less about 0.72. On the other hand, the values of the constant a are very much dependent on the dimensions of the modules and the other array configuration parameters. It seems that the present work is the only one which has made use of rectangular modules, while the other mentioned investigations used square ones. It can be concluded from this that when the rectangular modules are used in array configuration, they tend to enhance the heat transfer rate over that when square modules are used. For the present investigation the following correlation was obtained:

$$Nu_0 = 0.382Re^{0.72}. \tag{9}$$

The effects of changing the height of the module blocks in the fourth and fifth rows on the heat transfer characteristic of the uniform array configuration is shown in Fig. 5. The results are plotted in terms of the ratio of Nu of the array with different module heights, to that Nu_0 of the basic array configuration with uniform module array. When the height $H_1 > H_2$, the row by row Nu/Nu_0 distributions of the investigated step height ratio $(H_1 - H_2)/S = 1/8$ (where S is

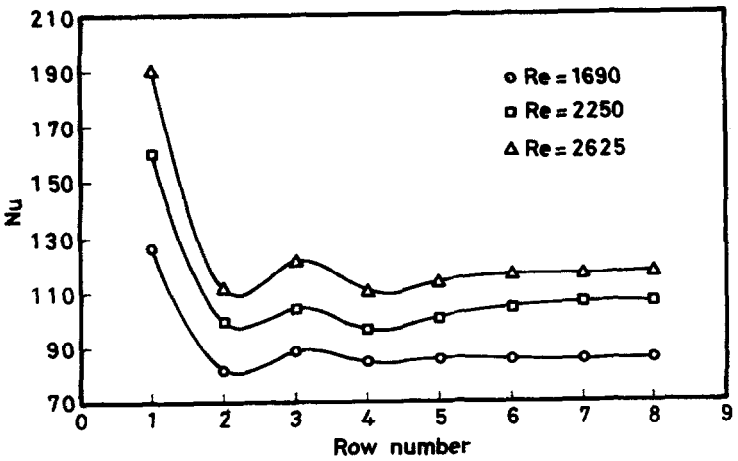

Fig. 3. Row by row of the per block Nusselt number distributions for the basic array configuration.

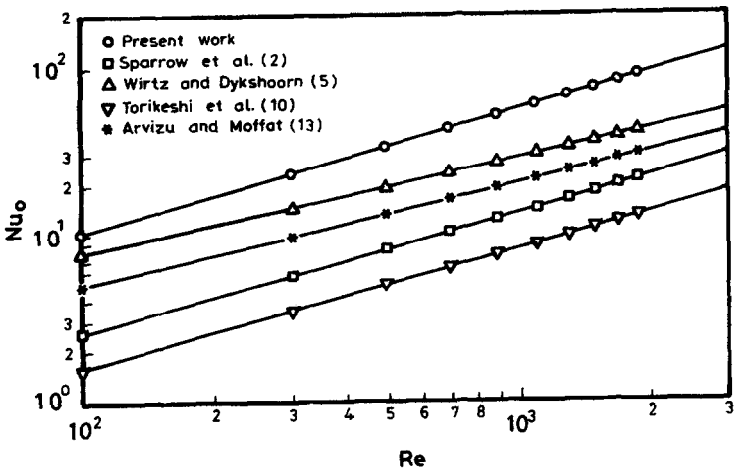

Fig. 4. Fully developed Nusselt number at various values of Reynolds number.

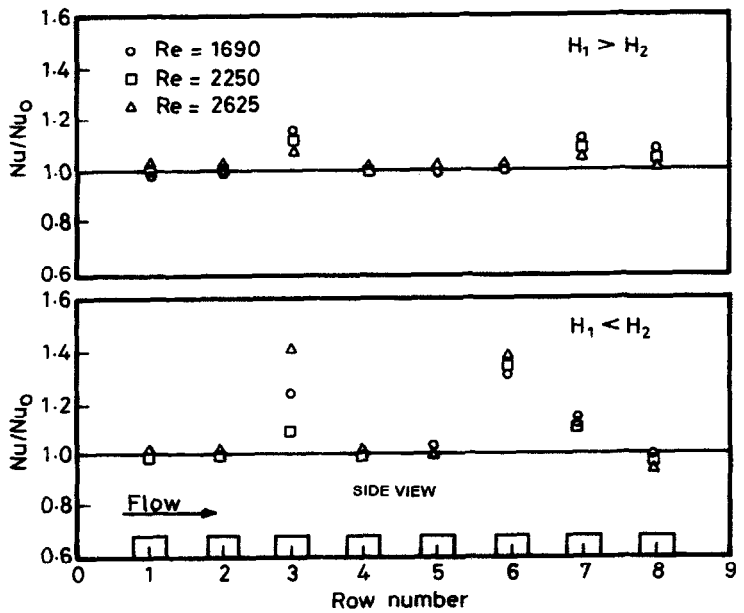

Fig. 5. Row by row Nusselt number at various values of module height.

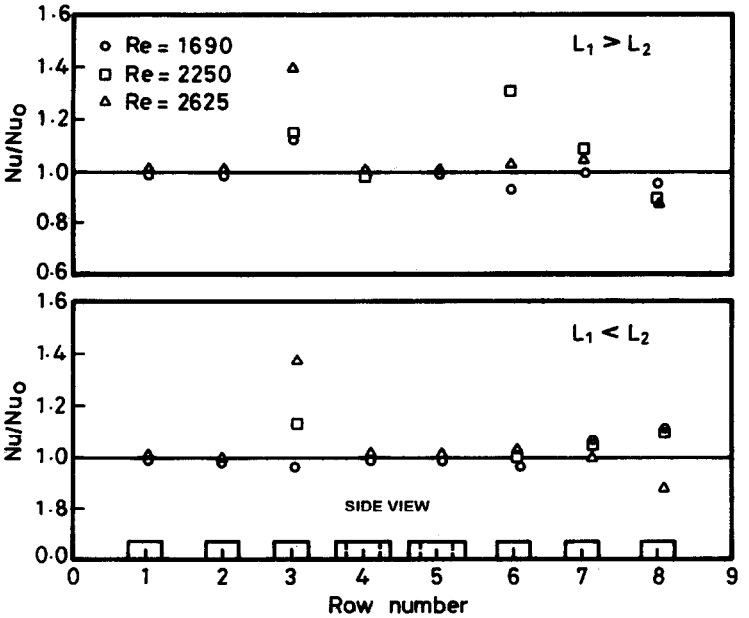

Fig. 6. Row by row Nusselt number at various values of module length.

the channel's height) indicate that for all Reynolds numbers investigated, the Nu/Nu_0 values increase with an increasing of the streamwise distance in the range from the fifth row to the eighth row, but with no enhancement at the sixth row. Also, an enhancement in the heat transfer coefficient occurs at the third row due to retardation of the flow at the fourth row. Furthermore, enhancement in the heat transfer coefficients is experienced at the seventh and eighth rows which could be attributed to the reattachment of the flow downstream of the fifth row of modules. The maximum enhancement occurs at the third and seventh rows, with a value of 14% at $Re = 1690$. Figure 5 also shows the results when $H_1 < H_2$ with maximum enhancements of 40 and 36% at $Re = 2625$ occurring at the third and sixth rows of the array, respectively. The enhancement at the third row may be attributed to the reverse flow that occurred between the fourth and the third rows, while the enhancement at the sixth row may be explained by the direct impingement of the air flow at this row of modules. It is interesting to note that Nu/Nu_0 decreases monotonically towards the fully developed value, downstream of the third row of the array.

The effect of changing the length of the modules in the direction of the flow on the Nusselt number is shown in Fig. 6. Two rows of modules were implanted at the fourth and fifth rows with a step length $(L_1 - L_2)/S = 1/8$. When $L_1 > L_2$, an enhancement in the heat transfer occurs in the third row for all values of Re. The maximum enhancement at the third row is 40% at $Re = 2625$ which is attributed to the increase in the circulation of air between the third and fourth rows. At the sixth row, the enhancement in the heat transfer rate is decreased to 32% at $Re = 2250$, while at the eighth row the heat transfer was attenuated. When $L_1 < L_2$ and the step length is $-1/8$, almost no enhancement was observed upstream of the fourth row, except for Re values of 2250 and 2625, where 39% enhancement occurred, which may be caused by the increase in turbulence between the two rows. However, as for the case of $L_1 > L_2$, attenuation of the heat transfer has occurred at the eighth row.

Figure 7 shows the Nu/Nu_0 distributions when the width of the modules at the fourth and fifth rows is varied. When $W_1 < W_2$ and the step width change is $-1/8$, the heat transfer enhancement occurs at the third and sixth rows for all Re values, due to the increase in the flow areas between the modules in the fourth and fifth rows, as well as the impingement of air at the sixth row. However, since these flow passages are blocked in the sixth and subsequent rows, the largest attenuation of 13% of the heat transfer occurred at the eighth row. On the other hand, when $W_1 > W_2$ with a step length of 2/8 and step width of 3/8, the results show that predominantly an attenuation of heat transfer has occurred at the third, seventh and eighth rows, respectively. A small enhancement in the heat transfer was observed at the sixth row.

It is interesting to note that the resultant changes in the heat transfer due to changing the height of the module in the fourth and fifth rows, always occur in other rows of the array, but never in rows 4 and 5 themselves. Although, no detailed flow measurements or flow visualizations have been carried out in the present investigation, one may attribute this to the changes that might have occurred in the flow structure, due to the change in size of the modules in these rows and which were only felt either downstream or upstream of them, as was explained before for the results shown in Figs. 5–7.

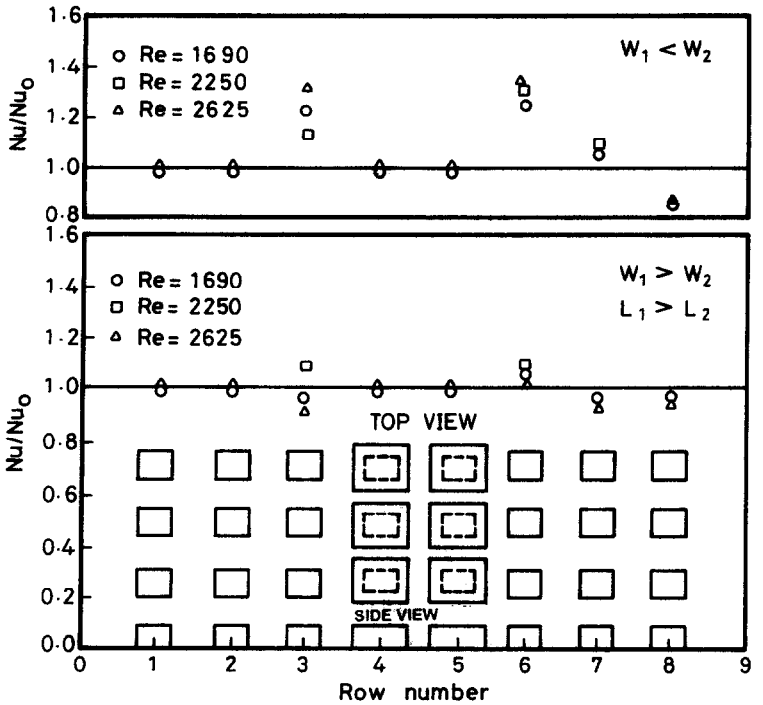

Fig. 7. Row by row Nusselt number at various values of module width.

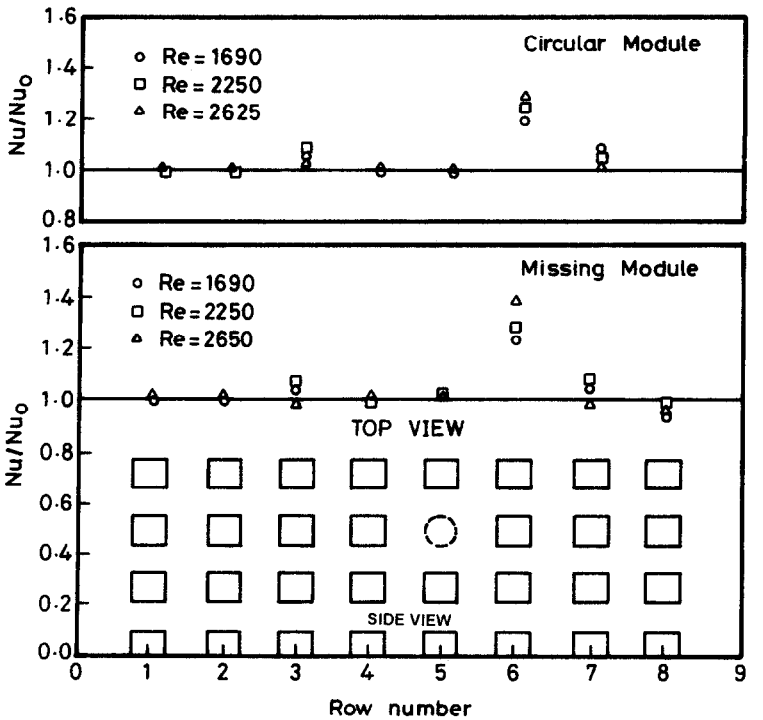

Fig. 8. Row by row Nusselt number of an array with a circular module or missing module.

In order to investigate the effect of a cylindrical shape transistor or a screw in the printed circuit board, an odd module of cylindrical shape was implanted in the fifth row of the array configuration. This cylindrical module is 20 mm in diameter and 10 mm in height. Figure 8 shows this effect, as well as the effect of the missing module. It can be seen from the figure that when a cylindrical module is implanted in the array configuration, a large enhancement in the Nusselt number of up to 28% is observed at the sixth row, and almost no enhancement occurs at the subsequent rows at the largest *Re* value, but rather an attenuation

in the heat transfer rate is observed at the eighth row. This test was also repeated when the odd cylindrical module was placed side by side along the active module. For such test, no significant enhancement of the heat transfer was noticed and consequently the results for this case are not presented.

Figure 8 also shows the Nu/Nu_0 distribution for the missing module array configuration, where one module was taken out from the fifth row of the basic array. It is interesting to note that the missing module tends to have higher effects on the heat transfer rate than the cylindrical module, as can be seen from the increase in the maximum enhancement in the heat transfer at the sixth row to 37%, compared with 28% for cylindrical module case. Attenuation in the heat transfer is again observed at the eighth row.

The temperature distribution of the modules along the test section in the direction of the flow was obtained by monitoring the temperature of the active module at the first row, as well as the temperature of the other passive modules downstream along the same column of the active module. It should be pointed out that the effect of the thermal wakes on the flanking columns has been observed to be negligible. Figure 9 presents the dimensionless temperature distribution along the test section, at the same column of the active module and at $Re = 1696$, compared with the results of Moffat *et al.* [7]. It can be seen that the effect of the thermal wake is felt at the first four to five rows downstream of the active module, with a similar trend to that observed by Moffat *et al.* [7]. The following correlation was obtained for the thermal wake and is applicable only to the one element immediately downstream from the heated module:

$$\theta_1 = 1.42Re^{-0.32}. \quad (10)$$

4.2. *Pressure drop results and discussion*

The effect of the presence of different size modules at the fourth and fifth rows of array configurations has been investigated and the obtained results of C_p/C_{po} are shown in Fig. 10, where C_p is the local pressure coefficient for the arrays with different size modules and C_{po} is the local pressure coefficient of the basic uniform array. It can be seen from the figure that whether the height or the length of the modules are changed the effect on the pressure drops is significant at the smallest Re value of 1690, especially when $L_1 < L_2$. When $H_1 > H_2$, as the flow crosses the fourth and fifth rows it tends to accelerate, and this gives rise to a sharp pressure drop. Just downstream of the fifth row, and as the flow expands and fills the available cross-section, a pressure recovery tends to take place. On the other hand, when $H_1 < H_2$ the opposite effect to that of $H_1 > H_2$ occurs. At the smallest value of Re, the implantation of shorter modules at the fourth and fifth rows tends to attenuate the pressure drop at the smallest value of Re. For the case when $L_1 > L_2$, attenuation in the pressure drop occurs almost at all rows for the smallest value of Re, while for the other values of Re the change in the pressure drop is very small. Now, when $L_1 < L_2$, all rows in the array experienced a reduction in the pressure drop, especially at $Re = 1690$.

The effect of changing the width of the modules at the fourth and fifth rows, the implantation of cylindrical module and the missing module case on the pressure drop is shown in Fig. 11. When $W_1 < W_2$, attenuation in the pressure drop is observed at the fourth and fifth row, as well as at the rows upstream of them. For the $W_1 > W_2$ array, almost similar trends to that of $W_1 < W_2$ are observed, except that at the fourth and fifth rows the pressure drop is increased. Furthermore, it can be seen from the figure that the implantation of a cylindrical module at the fifth row has a negligible effect on the pressure drop, except at a low Re value where the pressure drop has experienced almost constant attenuation. The missing module array has caused a small attenuation in the pressure

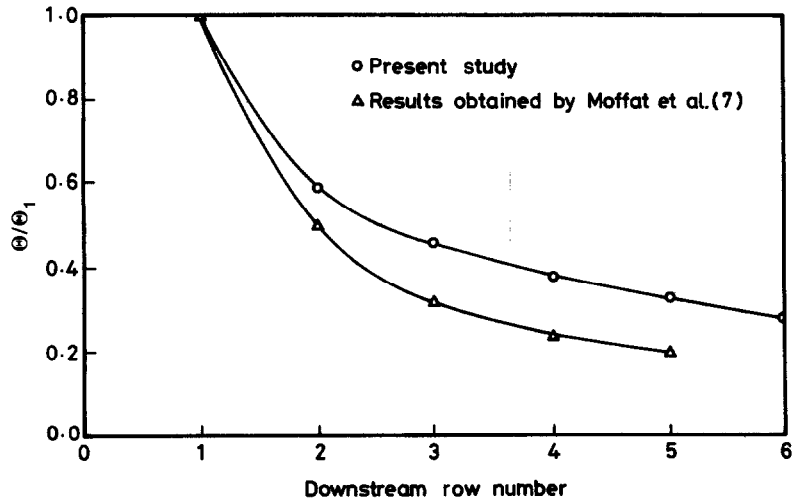

Fig. 9. Temperature distribution along a block column of modules downstream of the active module in the direction of the flow.

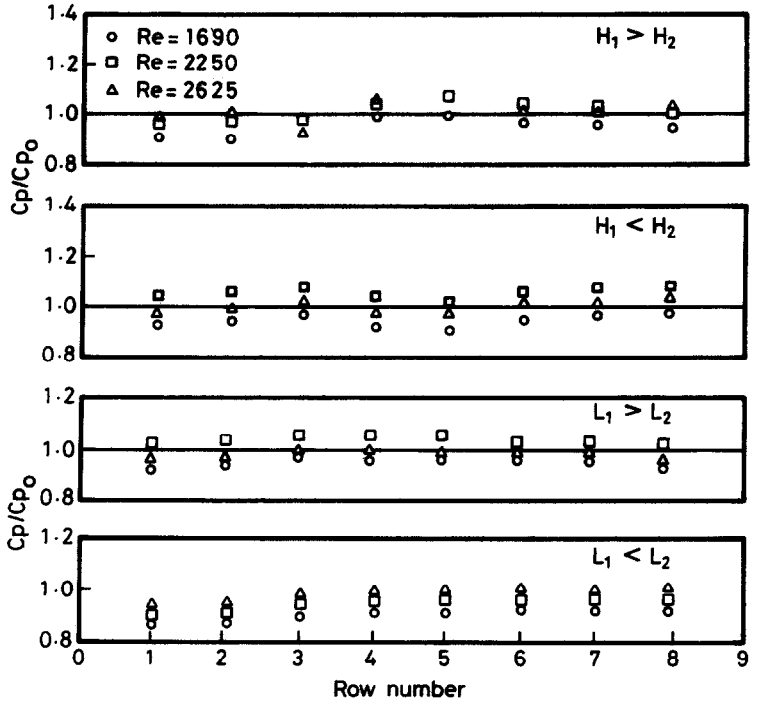

Fig. 10. Row by row pressure coefficient distributions at various values of module height and length.

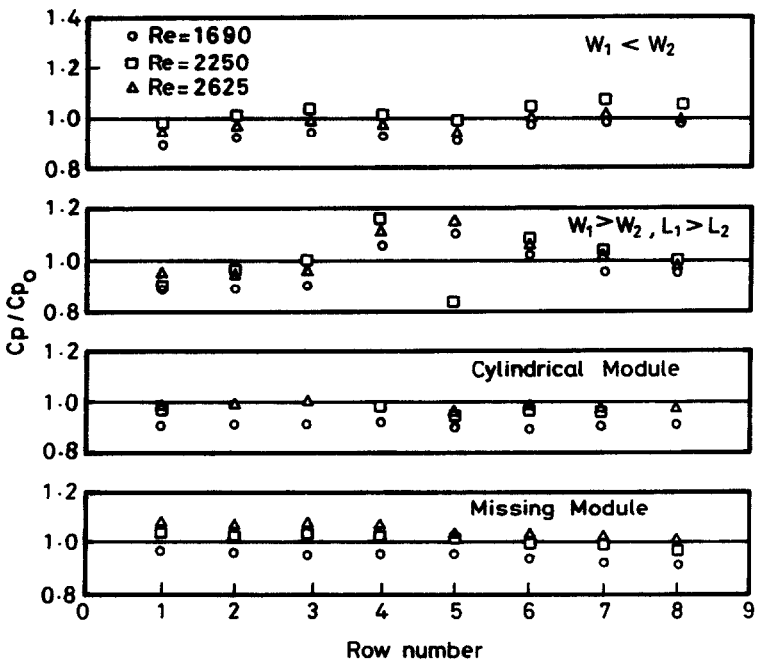

Fig. 11. Row by row pressure coefficient distributions at various values of module width, length, or the presence of a cylindrical module or missing module.

drop for all rows at the lowest value of Re, but for the highest value of Re the pressure drop is increased at the rows upstream of the fifth row, while downstream, the missing module effect on the pressure drop is negligible.

5. CONCLUSIONS

An experimental investigation was conducted to explore the effects of the size of the modules, as well as the presence of cylindrical module and missing module, on the heat transfer coefficient and pressure drop characteristics of array configurations composed of rectangular individual modules. The experimental results suggest the following conclusions:

(1) Using individual rectangular modules rather than square modules in the array configuration tends to enhance the heat transfer significantly. In general, the implantation of odd-size modules in the array is shown to be an effective means of heat transfer enhancement with a maximum enhancement value of 40%.

(2) If there is a missing module in the array, a maximum heat transfer enhancement of 37% occurs, where the missing nodule is just upstream of the module at which heat transfer coefficient is being monitored.

(3) The implantation of cylindrical module at the middle of an array configuration tends to enhance the heat transfer coefficient by as much as 28% at the next row downstream. However, no effect on heat transfer was observed when the cylindrical module was located side by side with the active module.

(4) The pressure drop results indicate that large size modules tend to enhance the pressure drop at their row locations by as much as 15%, while the cylindrical module tends to attenuate the pressure drop, especially at a low value of Reynolds number.

REFERENCES

1. M. L. Buller and R. F. Kilburn, Calculation of surface heat transfer coefficients for electronic module packages. In *Heat Transfer in Electronic Equipment*, HTD, Vol. 20, ASME Winter Annual Meeting, November pp. 15–29 (1981).
2. E. M. Sparrow, J. E. Niethammer and A. Chaboki, Heat transfer and pressure drop characteristics of array of rectangular modules in electronic equipment, *J. Heat Mass Transfer* **25,** 961–973 (1982).
3. E. M. Sparrow, S. B. Vemuri and D. S. Kadle, Enhanced and local heat transfer, pressure drop and flow visualization for arrays of block-like electronic components, *J. Heat Mass Transfer* **26,** 689–699 (1983).
4. E. M. Sparrow, A. A. Yanezmoreno and D. R. Otis, Convective heat transfer response to height differences in an array of block-like electronic components, *J. Heat Mass Transfer* **27,** 469–473 (1984).
5. R. A. Wirtz and P. Dykshoorn, Heat transfer from array of flatpacks in a channel flow, *Proceedings of Fourth Annual International Electronics Packaging Society*, Baltimore, pp. 318–326 (1984).
6. G. L. Lehmann and R. A. Wirtz, The effect of variations in streamwise spacing and length on convection from surface mounted rectangular components. In *Heat Transfer in Electronic Equipment*, (Edited by S. Oktay and R. J. Moffat), MTD-Vol. 48, 23rd National Heat Transfer Conference, Denver, Colorado, 4–7 August (1985).
7. R. J. Moffat, D. E. Arvizu and A. Ortega, Cooling electronic components: forced convection experiment with an air-cooled array. In *Heat In Electronic Equipment* (Edited by S. Oktay and R, J. Moffat) HTD-Vol 48, 23rd National Heat Transfer Conference, Denver, Colorado, 4–7 August (1985).
8. E. Ratts, C. H. Amon, B. B. Mikic and A. T. Patera, Cooling enhancement of forced convection air cooled chip array through flow modulation induced vortex shedding cylinders in cross-flow. In *Cooling Technology for Electronic Equipment* (Edited by Wing Aung), pp. 183–194. Hemisphere, Washington, DC (1988).
9. B. R. Hollworth and H. Fuller, Heat transfer and pressure drop in a staggered array of air-cooled components. In *Cooling Technology for Electronic Equipment* (Edited by Wing Aung), pp. 363–379. Hemisphere, Washington, DC (1988).
10. K. Torikoshi, M. Kawazoe and T. Kurihara, Convective heat transfer characteristics of arrays of rectangular blocks affixed to one wall of a channel. *ASME Natural and Mixed Convection in Electronic Equipment Cooling*, (Edited by R. A. Wirtz), HTD Vol. 100, The Winter Annual Meeting of American Society of Mechanical Engineering, Chicago, Il, 27 November–2 December (1988).
11. B. R. Hollworth and M. Durbin, Impingement cooling electronics, *ASME Trans. Engng Heat Transfer* **114,** 607–613 (1992).
12. S. J. Kline and F. A. McClintock, Describing uncertainties in single sample experiments, *Mech. Engng* **75,** 3–8 (1953).
13. D. E. Arvizu and R. J. Moffat, The use of superposition in calculating cooling requirements for circuit board mounted components. In *Proceedings of the 32nd Electronic Components Conference*, IEEE, EIA and CHMI, May (1982).